Hip Resurfacing Increases Bone Strains Associated with Short-Term Femoral Neck Fracture

Jason P. Long,[1] Thomas J. Santner,[2] Donald L. Bartel[3]

[1]University of Michigan, Ann Arbor, Michigan, [2]Ohio State University, Columbus, Ohio, [3]Cornell University, Ithaca, New York

Received 13 August 2008; accepted 22 February 2009
Published online 31 March 2009 in Wiley InterScience (www.interscience.wiley.com). DOI 10.1002/jor.20884

ABSTRACT: Short-term femoral neck fracture is a primary complication associated with contemporary hip resurfacing. Some fractures are associated with neck notching, while others occur in the absence of notching. These unexplained fractures may be due to large magnitude strains near the implant rim, which could cause bone damage accumulation and eventual neck fracture. We used statistically augmented finite element analysis to identify design and environmental variables that increase bone strains near the implant rim after resurfacing, and lead to strain magnitudes sufficient for rapid damage accumulation. After resurfacing, the compressive strains in the inferior, peripheral neck increased by approximately 25%, particularly when the implant shell was bonded. While the tensile strains in the peripheral neck were low in magnitude in the immediate postoperative models, they increased substantially following compressive damage accumulation. Low bone modulus, within the range of normal bone, and high head load contributed the most to large magnitude strains. Therefore, in some cases, hip resurfacing may cause a region of compressive bone damage to develop rapidly, which in turn leads to large tensile strains and potential neck fracture. Our study suggests that indications for surgery should account for bone material quality, and that rehabilitation protocols should avoid high-load activities. © 2009 Orthopaedic Research Society. Published by Wiley Periodicals, Inc. J Orthop Res 27:1319–1325, 2009

Keywords: hip resurfacing; finite element analysis; femoral neck fracture

The survivorship of hip resurfacing has improved but complications such as short-term neck fractures, which have an incidence of 1–2%,[1] still occur. While neck notching may increase the risk of neck fracture,[1,2] some fractures occur in the absence of notching.[3,4] In recent finite element (FE) analyses, it was observed that placing a stiff cobalt-alloy implant around the femoral head remnant unloaded this bone.[5,6] An additional consequence of hip resurfacing is increased bone strains near the rim of the shell, which is likely due to distal load transfer from the implant to the bone.[5] It is near the shell rim where fractures generally occur.[4]

Even in viable bone, damage can accumulate if the strains are sufficiently large (approximately −0.35% strain in compression and 0.25% strain in tension)[7,8] and applied repeatedly over a short time.[9] Therefore, cases may occur where bone has insufficient time to adapt to the altered loading environment, which could lead to fatigue fracture of the femoral neck. This is consistent with clinical studies where the mean time to resurfacing neck fracture was approximately 15 weeks,[1] which is less time than the duration of a complete bone remodeling cycle.[10]

Structural performance is a function of both design and environmental variables. Hip resurfacing design variables include the stem-bone geometry and the extent of fixation, and environmental variables include variations in bone structure, bone modulus, and joint loading. Environmental variables vary from individual to individual as well as within the same individual over time, and can be treated stochastically to describe a population of interest. Parametric FE analysis may be used to identify influential variables and improve survivorship through changes to implant design, patient selection criteria, and rehabilitation protocols.

Parametric studies using the FE method alone can be computationally prohibitive. An alternative approach is to use a computationally inexpensive, statistically based predictor of the FE model output, which is based on the structural response of the FE model to a small set of design and environmental variable combinations (training sites).[11] We used this approach to address two questions regarding short-term neck fracture. First, does hip resurfacing increase bone strains near the implant rim compared to the intact bone? Second, which design and environmental variables cause strains large enough such that rapid damage accumulation and neck fracture may occur?

MATERIALS AND METHODS

We analyzed the structural response, $y(x_d, x_e)$, of intact and resurfaced proximal femurs (Fig. 1). There were three design variables, x_d (S, the stem-hole geometry; F, the fixation of the implant shell; and μ, the stem-bone friction coefficient), and six environmental variables, x_e (B, a set of bones; W, a bone modulus parameter; θ_i and θ_o, the head load angles; H, the head load magnitude; and A, the abductor load magnitude). The function $y(x_d, x_e)$ was the output (true response) of the FE models, which was represented with the predictor response, $\hat{y}(x_d, x_e)$, based upon the true response at a limited number of variable combinations.[11]

FE Models

The implant was representative of several contemporary designs including the Birmingham (Smith and Nephew, Memphis, TN), the Conserve Plus (Wright Medical Technology, Arlington, TN), the Cormet (Stryker, Kalamazoo, MI), and the Durom (Zimmer, Warsaw, IN). The thickness of the cement mantle was 1 mm.[5] The stem diameter was 6 mm at its base and 65 mm long with the stem hole 2 mm longer than the stem to avoid load transfer at the tip. Two stem-hole geometries were analyzed: a 0.5° tapered stem in a 0.5° tapered hole (S_1), and a 0.5° tapered stem in a 6 mm diameter straight hole (S_2). A bonded shell (F_1) was represented using a displacement

Additional Supporting Information may be found in the online version of this article.

Correspondence to: J.P. Long (T: 734-647-1528; F: 734-647-0003; E-mail: longjp@umich.edu)

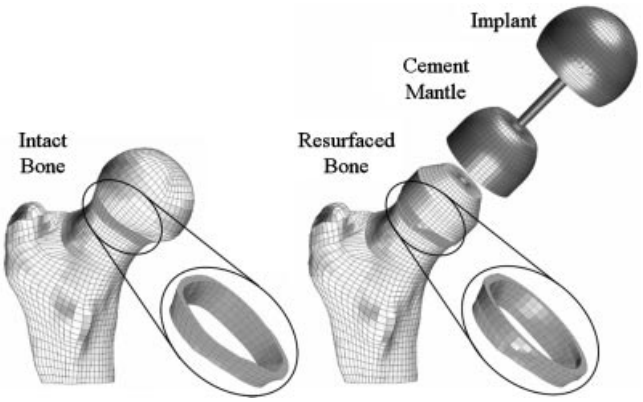

Figure 1. Intact and resurfaced finite element (FE) models were created using the same set of cadaveric femurs. For both the intact and resurfaced models, the region of interest was the peripheral neck at the implant rim.

compatible shell-cement interface, and an unbonded shell (F_2) was represented using a Coulomb friction interface with a coefficient of 0.5. The Coulomb friction coefficient along the stem-bone interface (μ) varied between 0.1 and 0.5.

Bone models were created using a single computed tomography (CT) scan of two cadaveric bones (S-Fig. 1). We determined three-dimensional bone geometry using image analysis and Studio (v4; Raindrop Geomagic, Durham, NC). Bone 1 (B_1) was from a 37-year-old male and Bone 2 (B_2) was from a 47-year-old male. Implant shell diameters were 50 mm for Bone 1 and 46 mm for Bone 2, which were the smallest diameter implants that did not violate the neck geometry. For both bones, the implant rim was located at the head-neck junction, and the stem axis was aligned with the neck axis because a valgus orientation[1,5] would have required violation of the neck in these bones. The FE meshes for all components of the intact and resurfaced models were generated using Truegrid (v2.2; XYZ Scientific Applications, Livermore, CA).

All elements (implant, cement, and bone) were assigned linear elastic, isotropic material properties with a Poisson's ratio of 0.3. The elastic moduli of the implant and cement were 200 GPa and 2 GPa, respectively. We calculated the elastic modulus for each bone element based upon the CT data. Using a family of curves (where individual curves were chosen using the scalar parameter W) we accounted for variations in the modulus-density relationship (Fig. 2A) that can arise from a number of sources, including differences in the sample population, anatomic location, and experimental testing methods. A single value of W was used for each analysis of the FE models. The bounding functions ($W = 0$ and $W = 1$) were based upon ultrasonically measured moduli from normal, human cancellous and cortical bone specimens from different anatomic sites.[12] Osteoporotic bone was not modeled, because patients with this disease would generally be poor candidates for hip resurfacing.[2] The bounding functions were determined as follows. For apparent densities less than 0.9 g/cm^3, the ranges of moduli were based upon experimentally derived confidence intervals. For apparent densities greater than 0.9 g/cm^3, the range of elastic moduli at an apparent density of 1.80 g/cm^3 was used to determine linear extrapolations of the confidence intervals.

The apparent density of each element was determined from the Hounsfield Units of the CT scan as follows. The bones were imaged without density phantoms. Therefore, to calibrate Hounsfield Units to apparent density, the average Hounsfield Units from the dense cancellous column within the femoral head, the cancellous bone in the greater trochanter, and the cortical diaphysis of each bone were assumed to have average apparent densities in those locations.[13,14] From these calibration points, we calculated a single regression curve of apparent density as a function of Hounsfield Units (S-Fig. 2). The apparent density of each element was calculated by interpolating the Hounsfield Units above and below the element centroid.

We verified the material model using the two bounding modulus-density functions with the intact bones and compared the computed strains to those determined in an in vitro study of

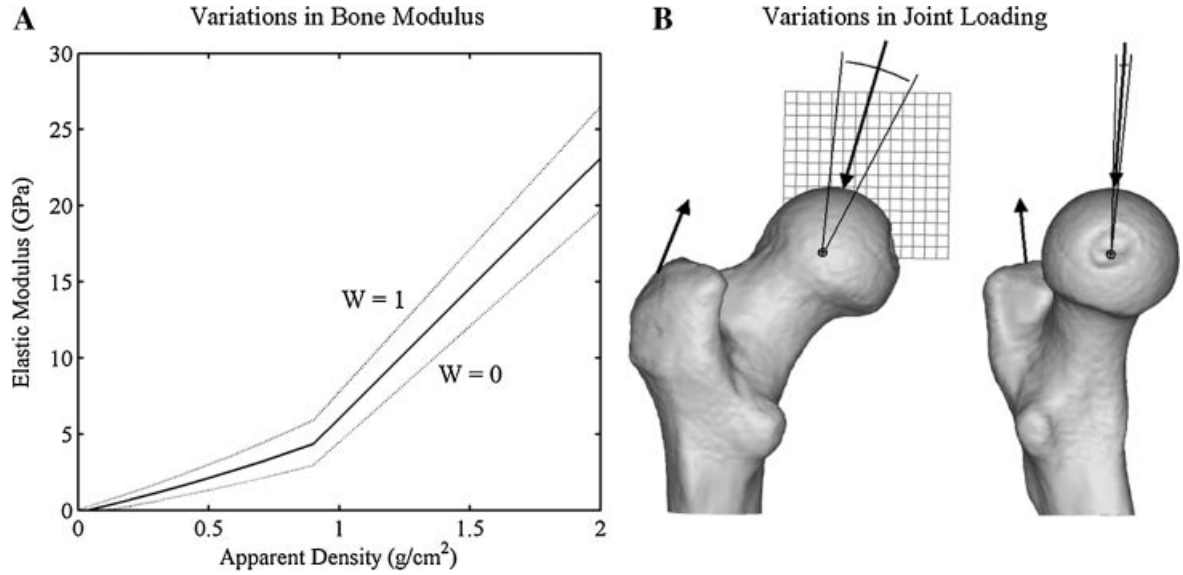

Figure 2. Variations in the elastic modulus–apparent density relationship were modeled using a scalar weighting parameter, W, that ranged between 0 and 1 (A). Variations in joint loading consisted of variations in head load direction, head load magnitude, and abductor load magnitude. Head load direction was described uniquely using in-plane and out-of-plane angles referenced to a regression plane. Positive in-plane load angles were less vertically oriented than load directions with negative angles; head load directions with positive out-of-plane load angles were more posteriorly oriented than load directions with negative angles.

five intact femurs.[15] The minimum principal (largest magnitude compressive) strains at the periosteal calcar ranged from −0.11−−0.21% strain for the FE models, which is consistent with the in vitro experiment (−0.10−−0.26%).

A variable representation of head and abductor loads was developed to account for intra- and interpatient variations in joint loading as well as the unknown joint loads from the donors of the modeled femurs (Fig. 2B). Uncertainties in loading were modeled using instrumented implant data from patients (average age 69 years, range 55–82) treated for osteoarthritis.[16,17] Three trials of peak head load during normal walking (approx. 4 km/h) were analyzed from each patient. We scaled head load magnitudes to account for kinetic differences between resurfacing and traditional hip replacement patient populations.[5] Accordingly, head load magnitudes were increased by 26%, which was the difference between the mean, peak abduction moment during walking for resurfacing patients[18] compared to the instrumented patients. This is a reasonable scaling factor because the instrumented patients had temporal agreement between peak abduction moment and peak head load, and the abduction moment was the primary joint moment component at this point in the gait cycle. The variations in head load direction were approximately planar (S-Fig. 3). Therefore, we fit a least-squared regression plane to the load vectors and described load direction using in-plane (θ_i) and out-of-plane (θ_o) angles. The in-plane angle and head load magnitude (H) had a strong correlation (S-Fig. 4A); out-of-plane angle was weakly correlated with in-plane angle and was considered an independent variable. We used the motion analysis data from the instrumented patients[17] and a force model of the hip[19] to calculate variations in abductor load magnitude (A). The calculated abductor and head load magnitudes were correlated (S-Fig. 4B).

We applied the head load through the implant center for the intact and resurfaced models. The head load was applied as a distributed force on the intact models and a nodal force on the resurfaced models. The abductor load was applied as a distributed force on the greater trochanter with a fixed line of action (0.39 medial, 0.058 anterior, 0.92 superior). All loads were based upon a nominal body weight of 800 N.[20,21] Models were constrained by fixing the distal end of the mesh.

Strain Measures

The structural response, $y(x_d, x_e)$, for the FE models was based upon strains calculated near the implant rim (Fig. 3). The region of interest (ROI) for both the intact and resurfaced models consisted of four adjacent, peripheral rings of bone elements: two inside the shell and two outside the shell (Fig. 1). This region was previously identified as a site of large magnitude strains after resurfacing.[5] Within the ROI, we determined the volume-weighted mean (VWM) strain by using the 10% of the ROI volume with the largest magnitude strains. The use of VWM strains ameliorates the limitations of modeling the cancellous bone as a continuum, particularly near interfaces, [22] and discounts localized strains that may not lead to damage accumulation. The VWM minimum principal (largest magnitude compressive) strain was calculated within the inferior half of the ROI and the VWM maximum principal (largest magnitude tensile) strain was calculated within the superior half of the ROI. Model solutions were calculated using ABAQUS (v6.5; ABAQUS, Inc., Providence, RI) and postprocessing was done in Patran (v2005; MSC Software, Santa Ana, CA).

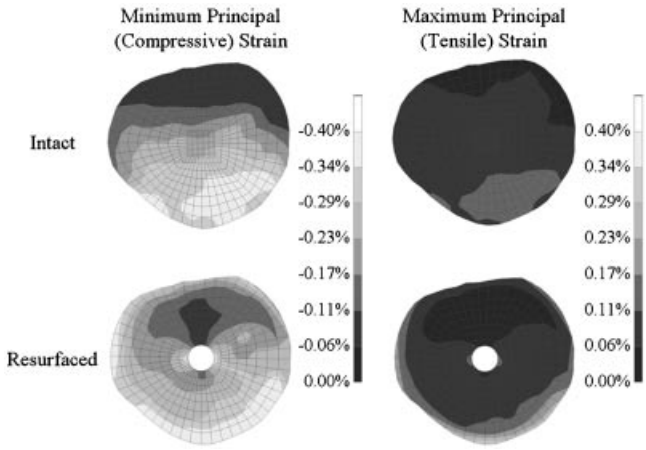

Figure 3. Cross-sections of the intact and resurfaced neck at the implant rim ($S = S_2$, $F = F_1$, $\mu = 0.11$, $B = B_1$, $W = 0.0067$, $\theta_i = 8.8^\circ$, $\theta_o = -1.1^\circ$, $H = 4.2$ BW, $A = 2.4$ BW) show an altered strain distribution after resurfacing. The external cross-sectional geometry of the neck did not change after resurfacing. The largest magnitude strains were located peripherally.

Statistical Analysis

We assigned ranges and distributions to each of the nine input variables (S-Table 1). Eighty variable combinations were selected according to a (space-filling) maximin Latin hypercube design, and the FE output, $y(x_d, x_e)$, was computed for each set of inputs. A rapidly computable interpolator, $\hat{y}(x_d, x_e)$, was constructed based on this 80 point training data. Our selected interpolator was a kriging predictor based on a Gaussian correlation function. This predictor can be viewed as an extension of regression-based predictors that has the additional property of interpolating the training data.[23,24] We

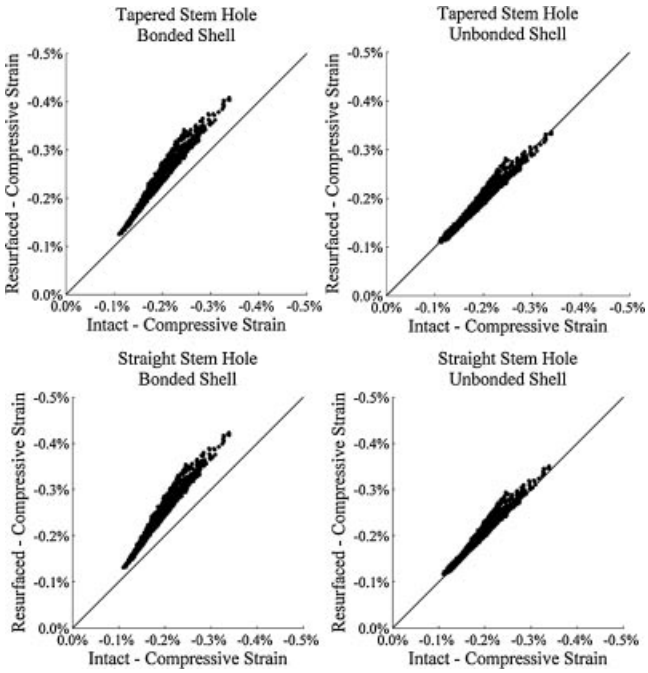

Figure 4. The four combinations of stem-hole geometry and shell fixation were compared at the same 2,000 combinations of environmental variables. The VWM compressive strains in the inferior portion of the peripheral neck generally increased in magnitude after resurfacing.

used JMP (SAS Institute, Cary, NC) and PErK (Dept. of Statistics, Ohio State University, Columbus, OH) software to calculate the predicted response.

From preliminary analysis, stem-hole geometry and shell fixation were the design variables that contributed the most to strain variability. Therefore, we used the predicted response to compare the VWM strains from the intact and resurfaced models at the four combinations of stem-hole geometry and shell fixation with the stem-bone friction coefficient held constant at 0.3; the environmental variables were varied over 2,000 combinations of the respective ranges and distributions. The predicted response was refined using 30 additional training sites from the resurfaced models and 10 from the intact models at combinations of variables with large magnitude strains. We calculated sensitivity indices (main effect of each input on the response) for each variable to assess their relative influence using GPM/SA (Los Alamos National Laboratory, Los Alamos, NM).[25] Additionally, main effect plots (trend of the response over the range of each input) were created for variables with large sensitivity indices.

Iterative Damage Model

We incorporated an iterative damage model into the resurfaced FE models to determine if compressive bone damage could increase the tensile strains within the superior, peripheral neck, because these large tensile strains likely increase the risk of neck fracture. From preliminary analysis, the VWM compressive strains in the inferior portion of the neck exceeded −0.35% strain in magnitude but only after resurfacing; the VWM tensile strains in the superior portion were always well below 0.25% strain. We based the damage model upon cycle-dependent, compressive fatigue damage. Each element was assigned a damage index (D) based on the Miner-Palmgren theory[26]:

$$D = \sum_{i=1}^{m} \left(\frac{n}{N_i} \right) \tag{1}$$

where D starts at zero (no damage) and could reach a value of one (completely damaged), N_i is the number of load cycles to failure at the ith strain level, n is the number of cycles per iteration, and m is the current iteration. The number of load cycles to failure (N_i) was calculated using

$$\log N_i = A \log \left(\frac{\varepsilon_i}{\varepsilon_y} \right) \tag{2}$$

where A is an experimentally determined parameter set to −9.21,[27] ε_i is the element's centroidal minimum principal strain at the ith iteration, and the ε_y is the yield strain (assumed to be 0.8% strain). Peak loads during gait were the only loads applied at each iteration. To represent a load cycle duration where fatigue damage dominates, the number of gait cycles per iteration (n) was 10,000.[8] When the damage index (D) reached 1, the element's modulus was reduced by 90% with no subsequent reduction. The damage model was applied to the entire femoral head remnant and neck, which is the bone most affected by the implant. This region was also away from locations where boundary conditions were applied to the bone such as the greater trochanter and distal cross-section. Iterations were ceased when the VWM tensile strain in the superior, peripheral neck reached 0.25% strain. Because we modeled damage accumulation that could lead to fracture, not fracture itself, the damage model iterations were stopped before substantial tensile damage accumulation could initiate and before neck fracture would occur. The iterative damage model was applied to several resurfaced FE models with VWM compressive strains ranging from −0.35−−0.46%, to determine the influence of initial strain on the number of iterations (gait cycles) required to reach the specified tensile strain.

RESULTS

The VWM compressive strains in the inferior half of the peripheral neck were substantially higher in magnitude and had greater variance than the VWM tensile strains in the superior half. Additionally, the compressive strains increased in magnitude by approximately 25% after resurfacing when the implant shell was bonded (Fig. 4). In some cases, strain magnitudes exceeded −0.35% strain after resurfacing. For the unbonded shell interfaces, the compressive strains changed little after resurfacing. When the stem hole was straight, the compressive strains were slightly higher in magnitude than when the stem hole was tapered. The tensile strains in the superior half of the peripheral did not increase after resurfacing, and ranged from 0.03–0.14% strain for all resurfaced models.

From the iterative damage model, compressive damage that started in the inferior, peripheral neck led to large tensile strains developing within the superior, peripheral neck (Fig. 5). The number of iterations depended upon the magnitude of the initial VWM compressive strain; only four iterations (40,000 gait cycles) were required when this strain was near −0.45%, and 12 or more iterations (at least 120,000 gait cycles) were required when this strain was near −0.35%. Most of the bone damage was localized near the implant rim.

The bone modulus parameter explained 67% of the variation in the VWM compressive strains for the resurfaced models, with large strains occurring at low (W near 0) values (Fig. 6). Additionally, head load

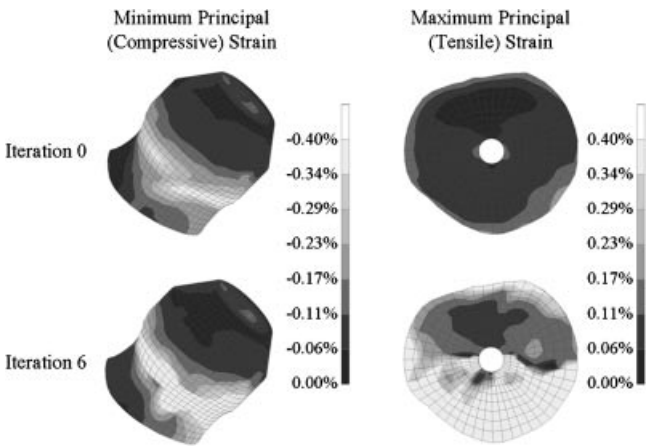

Figure 5. Surface and cross-sectional plots of principal strains show the effect of the iterative damage model. Before the start of the model (iteration 0), there is a localized region of large magnitude compressive strains near the rim of the implant shell. In this example, the initial VWM compressive strain was −0.40% strain, and six iterations (60,000 gait cycles) were required to reach a VWM tensile strain of 0.25% strain within the superior, peripheral neck. Large tensile strains that developed within the inferior portion of the neck were due to damage accumulation within this region.

magnitude explained 22% of the variation in compressive strains, with high head load producing large strains. Of the three design variables, shell fixation was the most influential, but accounted for only 3% of the variation in the compressive strains.

DISCUSSION

Using a statistically augmented FE analysis that accounted for variations in design and environmental variables, we found that in the immediate postoperative state hip resurfacing increased the magnitude of the compressive strains in the inferior half of the peripheral neck near the implant rim by approximately 25%, particularly when the implant was bonded. In some cases, these strains exceeded −0.35% after resurfacing. In contrast, the tensile strains in the superior half of the peripheral neck changed little in the immediate postoperative models and were low in magnitude. However, the tensile strains increased substantially following compressive damage accumulation that initiated within the inferior, peripheral neck. While femoral neck fracture was not modeled, the increased tensile strains would likely increase the potential for fracture. We also identified low bone modulus, within the range of normal bone, and high head load magnitude as the primary variables that led to strains that may be sufficient for rapid damage accumulation within the femoral neck.

The bonded and unbonded interface conditions likely provide upper and lower bounds to in vivo systems because partial debonding may occur. Bonded interfaces maximize implant stability, while an unbonded implant is inherently unstable. Therefore, even though the strains associated with the bonded implant were larger in magnitude than those for the unbonded implant, implant stability remains critical for successful clinical outcomes.

Bone is a damage-accumulating material, but damage from normal, physiological loading is kept in check by the bone remodeling process.[9,28] Short-term neck fractures (mean time of approximately 15 weeks)[1] commonly occur before remodeling can prevent substantial damage accumulation.[10] The rate of bone damage accumulation is highly sensitive to strain magnitude.[7,8,27] For example, increasing the strain due to resurfacing as seen in our results (25%) can multiply the rate of damage accumulation several times or even an order of magnitude. This is supported by the threefold decrease in the number of damage model iterations needed to reach the tensile threshold strain when the initial compressive strain magnitude was increased from −0.35−−0.45%. While the tensile and compressive strain thresholds used in this study represent values where rapid damage accumulation within the bone could occur,[7,8] physiologically there would be complex interactions between damage and repair processes that would lead to variations in these thresholds. Nevertheless, in some cases after resurfacing, strains are likely large enough to rapidly reduce the structural stiffness of the neck and eventually cause fracture. This mechanism is similar to stress fractures suffered by competitive athletes and military recruits,[29] which can lead to displaced fracture in some cases.[30] Furthermore, hip resurfacing patients are generally more active than traditional hip replacement patients,[31] and bone damage may accumulate if a patient's activity level were to be too great during the rehabilitation period.

An alternative explanation is that osteonecrosis is primarily responsible for resurfacing neck fracture in the absence of notching.[32] The incidence of osteonecrosis following fracture, however, has been low in multicenter retrieval studies.[3,4] Additionally, the degradation of bone material properties linked to osteonecrosis is likely caused by accumulating bone damage unchecked by bone remodeling.[28] In cases of short-term neck fracture, even viable bone could not undergo substantial remodeling and repair during the time between surgery and fracture.

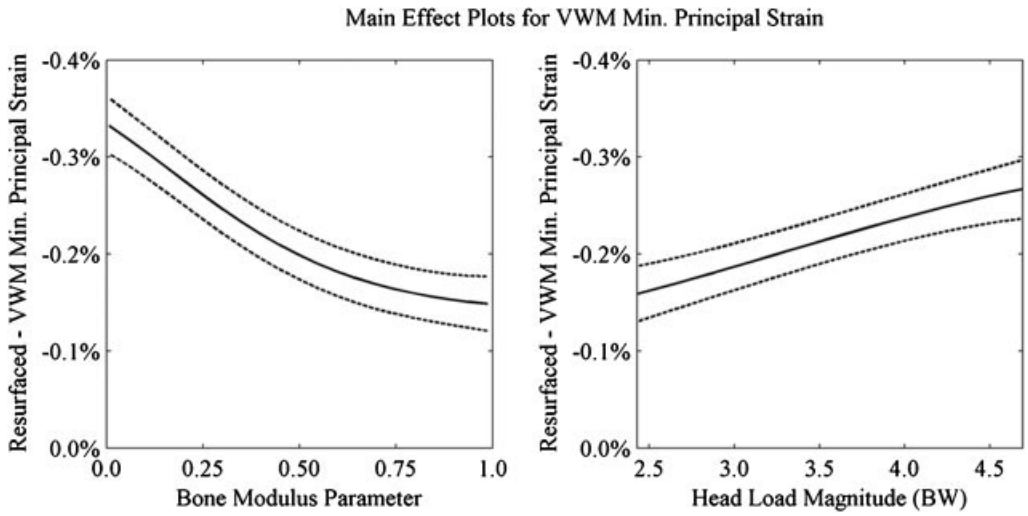

Figure 6. Low bone modulus and high head load primarily contributed to large compressive strains. The solid lines represent the mean function and dotted lines represent 95% confidence curves.

Parametric studies using FE analysis are computationally expensive, but we efficiently analyzed thousands of combinations of variables using a statistical predictor based on FE output. Our results are consistent with clinical findings. For example, large compressive strains associated with rapid damage accumulation were observed in a small subset of the variables examined, which is consistent with the 1–2% clinical incidence of short-term neck fracture.[1] Additionally, the importance of bone modulus is consistent with clinical findings that indicate low bone density is a risk factor for resurfacing neck fracture.[2]

The results of our study must be interpreted in terms of the methods we used. First, FE models, like all structural analyses and in vitro experiments, only approximate the in vivo system. While many combinations of design and environmental variables were incorporated into our analysis, the results are dependent upon how well the bone, implant, and boundary conditions were modeled. Therefore, our results should be interpreted primarily in terms of the general effects and relative influence of the variables analyzed. Second, bone structure varies from individual to individual and within an individual over time. We modeled only two representative bones, but their structural behavior was similar, indicating that the general results of our study are not specific to an individual bone. Third, holes are commonly drilled into the head remnant to allow cement to penetrate into the bone. The cement-bone composite was not incorporated in our FE models, but the material properties of the native bone and cement are similar in magnitude, and we would expect little change in the strains if the composite were modeled. Finally, the iterative damage model only incorporated compressive fatigue and did not incorporate other processes that might accelerate damage accumulation (e.g., creep and crack propagation). The iterative model also did not include bone remodeling, but an early phase of this process is osteoclastic resorption, which would increase bone porosity, leading to further increased strains and rate of damage accumulation.[29] Therefore, the results from the iterative model likely provide a lower limit to the rate of damage accumulation during the immediate postoperative period.

In summary, we found that hip resurfacing increased the compressive strains within the inferior half of the peripheral neck. Using a fatigue-based damage model, accumulated damage reduced the structural stiffness of the femoral neck. This resulted in increased tensile strains in the superior neck that could eventually lead to neck fracture. Therefore, we believe that short-term neck fracture, in the absence of notching, may be a consequence of rapid damage accumulation near the implant rim. Additionally, we found that low bone modulus, within the range of normal bone, and high head load magnitude were the primary variables that contributed to large magnitude strains. Our work provides a mechanistic framework with important clinical implications for why these variables may affect fracture in the absence of neck notching. Others have found that measures of bone material quality affect the risk for short-term neck fracture.[2,33] Therefore, we agree with these investigators that bone material quality should be assessed when screening patients for hip resurfacing. Furthermore, many hip resurfacing patients take part in strenuous activities,[31] and may be inclined to pursue aggressive rehabilitation protocols that could result in large head loads. Our results suggest that high-load activities should be avoided during rehabilitation.

ACKNOWLEDGMENTS

We thank Gang Han and Kirk Gunsallus for their assistance in model development and data processing. We also thank Dr. Edwin Su for his insight and a demonstration of surgical technique. This work was supported in part by the National Science Foundation under Agreement No. 0635561. The authors also received support from the Clark and Kirby Foundations as well as institutional research funds from Zimmer, Inc., for projects of mutual interest.

REFERENCES

1. Anglin C, Masri BA, Tonetti J, et al. 2007. Hip resurfacing femoral neck fracture influenced by valgus placement. Clin Orthop Relat Res 465:71–79.
2. Shimmin AJ, Bare J, Back DL. 2005. Complications associated with hip resurfacing arthroplasty. Orthop Clin North Am 36:187–193.
3. Campbell P, Beaule PE, Ebramzadeh E, et al. 2006. A study of implant failure in metal-on-metal surface arthroplasties. Clin Orthop Relat Res 453:35–46.
4. Morlock MM, Bishop N, Ruther W, et al. 2006. Biomechanical, morphological, and histological analysis of early failures in hip resurfacing arthroplasty. Proc Inst Mech Eng [H] 220: 333–344.
5. Long JP, Bartel DL. 2006. Surgical variables affect the mechanics of a hip resurfacing system. Clin Orthop Relat Res 453:115–122.
6. Ong KL, Kurtz SM, Manley MT, et al. 2006. Biomechanics of the Birmingham hip resurfacing arthroplasty. J Bone Joint Surg Br 88B:1110–1115.
7. Moore TL, Gibson LJ. 2003. Fatigue of bovine trabecular bone. J Biomech Eng 125:761–768.
8. Pattin CA, Caler WE, Carter DR. 1996. Cyclic mechanical property degradation during fatigue loading of cortical bone. J Biomech 29:69–79.
9. Martin RB. 2003. Fatigue microdamage as an essential element of bone mechanics and biology. Calcif Tissue Int 73: 101–107.
10. Parfitt AM, Mundy GR, Roodman GD, et al. 1996. A new model for the regulation of bone resorption, with particular reference to the effects of bisphosphonates. J Bone Miner Res 11:150–159.
11. Sacks J, Welch WJ, Mitchell TJ, et al. 1989. Design and analysis of computer experiments. Stat Sci 4:409–423.
12. Rho JY, Ashman RB, Turner CH. 1993. Young's modulus of trabecular and cortical bone material: ultrasonic and microtensile measurements. J Biomech 26:111–119.
13. Morgan EF, Keaveny TM. 2001. Dependence of yield strain of human trabecular bone on anatomic site. J Biomech 34:569–577.

14. Snyder SM, Schneider E. 1991. Estimation of mechanical properties of cortical bone by computed tomography. J Orthop Res 9:422–431.
15. Oh I, Harris WH. 1978. Proximal strain distribution in the loaded femur: an in vitro comparison of the distributions in the intact femur and after insertion of different hip-replacement femoral components. J Bone Joint Surg Am 60A:75–85.
16. Bergmann G, Graichen F, Rohlmann A. 1993. Hip joint loading during walking and running, measured in two patients. J Biomech 26:969–990.
17. Bergmann G, Deuretzbacher G, Heller M, et al. 2001. Hip contact forces and gait patterns from routine activities. J Biomech 34:859–871.
18. Mont MA, Seyler TM, Ragland PS, et al. 2007. Gait analysis of patients with resurfacing hip arthroplasty compared with hip osteoarthritis and standard total hip arthroplasty. J Arthroplasty 22:100–108.
19. Paul JP. 1967. Force transmitted by joints in the human body. Proc Inst Mech Eng 181:8–15.
20. Amstutz HC, Beaule PE, Dorey FJ, et al. 2004. Metal-on-metal hybrid surface arthroplasty: two to six-year follow-up study. J Bone Joint Surg Am 86A:28–39.
21. Daniel J, Pynsent PB, McMinn DJ. 2004. Metal-on-metal resurfacing of the hip in patients under the age of 55 years with osteoarthritis. J Bone Joint Surg 86B:177–184.
22. Harrigan TP, Jasty M, Mann RW, et al. 1988. Limitations of the continuum assumption in cancellous bone. J Biomech 21: 269–275.
23. Forrester AIJ, Sóbester A, Keane AJ. 2008. Surrogate models in engineering design: a practical guide. Chichester: J. Wiley. 210 p.
24. Santner TJ, Williams BJ, Notz W. 2003. The design and analysis of computer experiments. 1st edn. New York: Springer. 283 p.
25. Oakley JE, O'Hagan A. 2004. Probabilistic sensitivity analysis of complex models: a Bayesian approach. J R Statist Soc B 66:751–769.
26. Carter DR, Caler WE. 1985. A cumulative damage model for bone fracture. J Orthop Res 3:84–90.
27. Haddock SM, Yeh OC, Mummaneni PV, et al. 2004. Similarity in the fatigue behavior of trabecular bone across site and species. J Biomech 37:181–187.
28. Schaffler MB. 2003. Role of bone turnover in microdamage. Osteoporos Int 14:73–80.
29. Burr DB, Forwood MR, Fyhrie DP, et al. 1997. Bone microdamage and skeletal fragility in osteoporotic and stress fractures. J Bone Miner Res 12:6–15.
30. Stoneham MD, Morgan NV. 1991. Stress fractures of the hip in Royal Marine recruits under training: a retrospective analysis. Br J Sports Med 25:145–148.
31. Naal FD, Maffiuletti NA, Munzinger U, et al. 2007. Sports after hip resurfacing arthroplasty. Am J Sports Med 35:705–711.
32. Little JP, Taddei F, Viceconti M, et al. 2007. Changes in femur stress after hip resurfacing arthroplasty: response to physiological loads. Clin Biomech 22:440–448.
33. Schmalzried TP, Silva M, de la Rosa MA, et al. 2005. Optimizing patient selection and outcomes with total hip resurfacing. Clin Orthop Relat Res 441:200–204.